APPLICATION NOTE

Low-moment Measurements with the Model 8600 VSM

B. C. Dodrill, C. Radu, Lake Shore Cryotronics

Abstract

The most commonly used magnetometric technique to characterize magnetic materials is vibrating sample magnetometry (VSM).[1] A VSM system can measure magnetically soft (low coercivity) and hard (high coercivity) materials in many forms: solids, powders, single crystals, thin films, or liquids. It can be used to perform measurements from low to high magnetic fields employing electomagnets, or high-field superconducting magnets. It can be used to perform measurements from very low to very high temperatures with an integrated cryostat or furnace. A VSM system possesses a dynamic range extending from 10^{-8} emu (10^{-11} Am^2) to above 10^3 emu (1 Am^2), enabling it to measure materials that are both weakly magnetic (thin films, nanoscale structures, etc.) and strongly magnetic (permanent magnets).

In this application note, we will discuss the sensitivity of the 8600 Series VSM systems and present very low-moment measurement results at ambient temperature.

Lake Shore CRYOTRONICS

VSM sensitivity

Some magnetic materials, such as nanowires, nanoparticles, thin films, etc., typically possess weak magnetic moments owing to the small amount of magnetic material present. Thus, the sensitivity of a VSM is an important consideration as it determines the smallest magnetic moment that can be measured with acceptable signal-to-noise. The ultimate noise floor of the 8600 Series VSM is 1.5×10^{-8} emu (1.5×10^{-11} Am^2) or 15 nemu.

In a VSM, the voltage induced in the sensing coils is given by:

$$V_{emf} = mAfS \qquad \text{Equation 1}$$

m = magnetic moment

A = amplitude of vibration

f = frequency of vibration

S = sensitivity function of the VSM sensing coils

S is determined by calibrating the VSM with a magnetic calibrant,[2] i.e., a material with known magnetization at a specified applied field H.

A VSM's sensitivity depends on several factors:

- Electronic sensitivity
- Noise rejection through signal conditioning
- Amplitude and frequency of mechanical drive
- Thermal noise of sensing coils
- Optimized design and coupling (proximity) of sensing coils to the sample under test
- Vibration isolation of the mechanical head assembly from the electromagnet and VSM sensing coils
- Minimization of environmental mechanical and electrical noise sources, which can deleteriously effect VSM sensitivity

It is clear from Equation 1 that increasing A, f, or S will improve moment sensitivity; however, there are practical limitations to each. Frequencies of less than ~100 Hz are typically used to minimize eddy current generation in magnetic materials that are electrically conductive, and it is also important to avoid frequencies that are close to the line frequency and its higher-order harmonics.

The vibration amplitude should be sufficiently small to ensure that the sample is not subjected to inhomogeneous magnetic fields arising from the field source. S may be increased by optimizing the design of the sensing coils (i.e., number of windings, coil geometry, etc.), and by increasing the coupling between the sense coils and the sample under test (i.e., minimize gap spacing). At first glance, it would seem that all that one needs to do to increase S is to maximize the number of windings in the coils, however, this increases the resistance of the coils which, in turn, increases their thermal noise and negatively impacts their signal-to-noise. Finally, increasing signal averaging of the lock-in amplifier (LIA) used to measure the voltage induced in the sensing coils also improves signal-to-noise.

There are three 8600 VSM models—8604, 8607, and 8610 employing varible-gap 4 in, 7 in, and 10 in electromagnets. Each has four gap settings, two for room temperature measurements (gaps 1 and 2), and two for variable-temperature measurements: gap 3 (86-SSVT, 78 K to 950 K) and gap 5 (86-CRYO, 4.2 K to 450 K and 86-OVEN, 300 K to 1273 K). The table below shows the maximum applied fields and sensitivity (RMS noise at 10 s/pt averaging) at each gap setting for each of the 8600 models.

Maximum applied fields and sensitivity (RMS noise at 10 s/pt averaging)

Gap setting	Pole gap	Max. sample space	8604**	8607**	8610**	Noise floor***
1 – RT	7.5 mm	3.5 mm*	27.6 kOe (2.76 T)	32.2 kOe (3.22 T)	36.2 kOe (3.62 T)	15 nemu
2 – RT	12 mm	8 mm*	25.2 kOe (2.52 T)	29.8 kOe (2.98 T)	33.7 kOe (3.37 T)	30 nemu
3 – SSVT	20 mm	16 mm*	20.3 kOe (2.03 T)	26.0 kOe (2.60 T)	29.8 kOe (2.98 T)	90 nemu
5 – CRYO/OVEN	28 mm	24 mm*	15.5 kOe (1.55 T)	22.7 kOe (2.27 T)	26.3 kOe (2.63 T)	300 nemu

* *Sample size 6.4 mm with VT options.*

** *Values are with the high-field (HF) FeCo pole caps, optional with the 8604 and 8607, standard with the 8610.*

*** *10 s averaging.*

Figures 1a and 1b show typical noise measurement results at 100 ms/pt (1a) and 10 s/pt (1b) averaging. Note that the vertical axis is expressed in nemu = 10^{-9} emu (10^{-12} Am^2). The RMS noise values are noted in the figure captions.

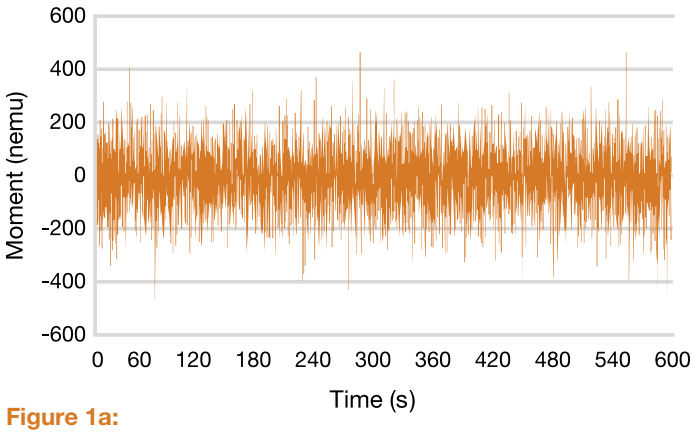

Figure 1a:
Noise measurement results at 100 ms/pt averaging. The observed noise is 119.5 nemu (11.95 x 10^{-11} Am^2).

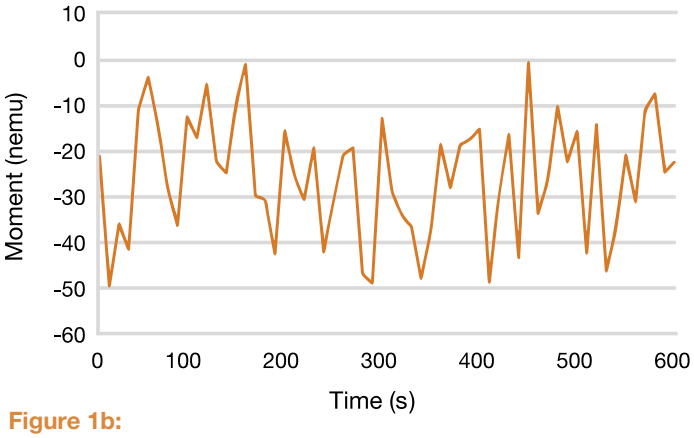

Figure 1b:
Noise measurements results at 10 s/pt averaging. The observed noise is 13 nemu (1.3 x 10^{-11} Am^2)

Low-moment measurements at room temperature (gaps 1 and 2)

A. 5.8 µemu (5.8 × 10^{-9} Am^2) CoPt thin film (gap 1):

Figure 2 shows typical major hysteresis loop (MHL) results recorded at gap 1 at 0.5 s averaging. The MHL was recorded to ±5 kOe (0.5 T) in equal field increments of 25 Oe (2.5 mT). Both measured and linearly corrected (i.e., to remove the diamagnetic contribution arising from both the sample holder and film substrate) MHLs are shown. Figure 3 shows linearly corrected MHLs at 0.5 and 1 s averaging to illustrate the impact of signal averaging on signal-to-noise. Note that full scale in Figure 3 is only ±6 µemu (6 × 10^{-9} Am^2).

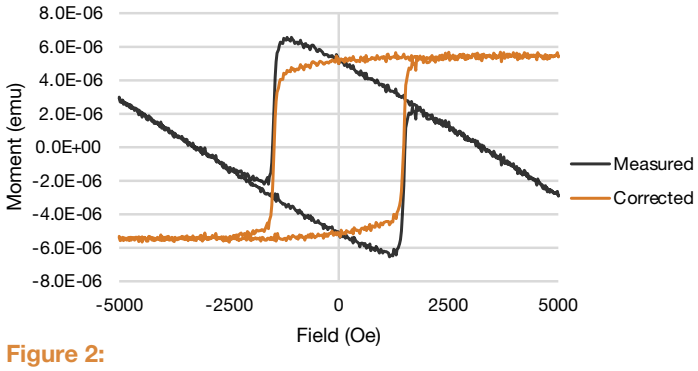

Figure 2:
CoPt MHL at 0.5 s averaging (measured and linearly corrected).

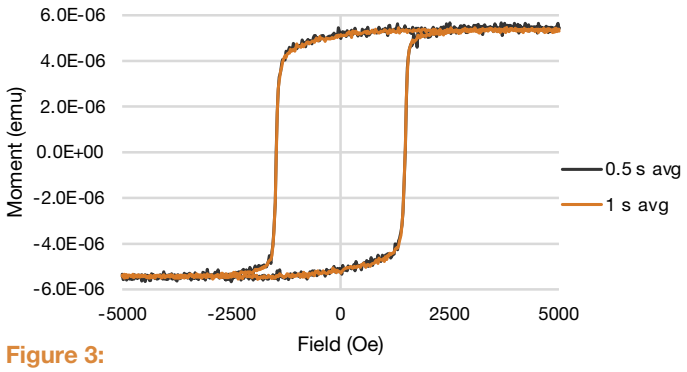

Figure 3:
CoPt MHLs (linearly corrected) at 0.5 and 1 s averaging.

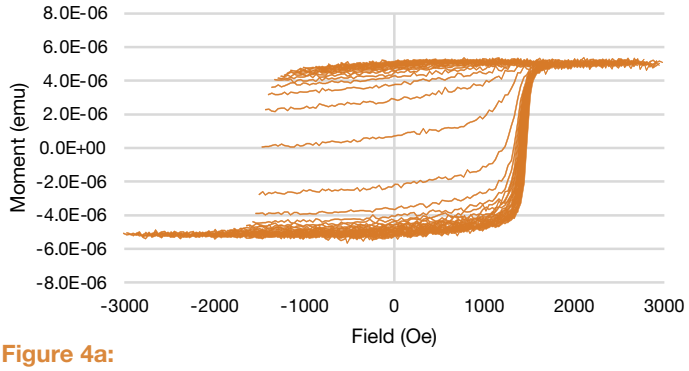

Figure 4a:
Measured FORC for the 5.8 µemu CoPt thin film sample at 0.5 s averaging.

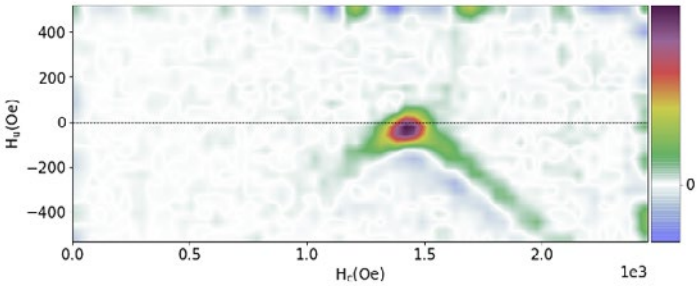

Figure 4b:
FORC diagram for the 5.8 µemu CoPt thin film.

While the most common measurement used to characterize a material's magnetic properties is measurement of the major hysteresis loop (MHL), more complex magnetization curves covering states with field and magnetization values located inside the major hysteresis loop, such as minor hysteresis loop and first-order reversal curve (FORC) measurements,[3,4] can give additional information that can be used for characterization of magnetic interactions.

A FORC measurement is relevant to any magnetic material composed of fine (micron- or nano-scale) magnetic particles. It has been extensively applied to geological materials,[5,6] magnetic nanostructures,[7] thin films,[8] permanent magnets,[9] multiphase magnetic systems,[10] magnetocaloric materials,[11] and a host of other magnetic materials.

A FORC is measured by saturating a sample in a field H_{sat}, decreasing the field to a reversal field H_a, then measuring moment versus field H_b as the field is swept back to H_{sat}; this process is repeated for many values of H_a yielding a series of FORC. The FORC distribution $\rho(H_a, H_b)$ is the mixed second derivative:

$$\rho(H_a, H_b) = -(1/2)\partial^2 M(H_a, H_b)/\partial H_a \partial H_b$$

A FORC diagram is a 2D or 3D contour plot of $\rho(H_a, H_b)$. It is common to change the coordinates from (H_a, H_b) to: $H_c = (H_b - H_a)/2$, $H_u = (H_b + H_a)/2$.

H_u represents the distribution of interaction or reversal fields, and H_c represents the distribution of switching or coercive fields of the hysterons. There are a number of open-source FORC analysis software packages, such as FORCinel[12] and VARIFORC.[13] In the results that follow, Lake Shore's RTForc™ software[14] was used to calculate the FORC distribution and plot the FORC diagram.

Noise floor and sensitivity are particularly of interest for FORC measurements because the number of points acquired in a typical measurement is 10× more than is typically recorded in a simple hysteresis loop. Having the lowest noise floor available in an electromagnet-based VSM, the 8600 Series does not require long signal averages to obtain good signal-to-noise, even for low-moment samples, which equates to shorter FORC measurement times. This combined with the high field ramp rates attainable with electromagnets $(10\ kOe/s = 1\ T/s)$ makes the 8600 the best-suited tool for FORC measurements.

Figures 4a and 4b show a typical series of FORC and the corresponding FORC diagram for the 5.8 µemu CoPt thin film. The FORC parameters were: $H_{sat} = 10\ kOe\ (1\ T)$, $\pm H_u = 500\ Oe\ (50\ mT)$, $H_c = 2.5\ kOe\ (0.25\ T)$, $N = 101$, field increment $\Delta H = 25\ Oe\ (2.5\ mT)$. The FORC were measured at 0.5 s averaging.

B. 1.5 µemu (1.5 × 10^{-9} Am^2) Fe-doped (0.5%) SiN ceramic sphere (2 mm diameter; gap 1):

Figure 5 shows the MHL recorded at gap 1 to ±5 kOe (0.5 T) in equal field increments of 25 Oe (2.5 mT). Both measured and linearly corrected (i.e., to remove the diamagnetic contribution arising from both the sample holder and the SiN) MHLs are shown. Figure 6 shows the linearly corrected MHLs at 2 and 5 s averaging to illustrate the impact of signal averaging on signal-to-noise. Note that full scale in Figure 6 is only ±2 µemu (2 × 10^{-9} Am^2).

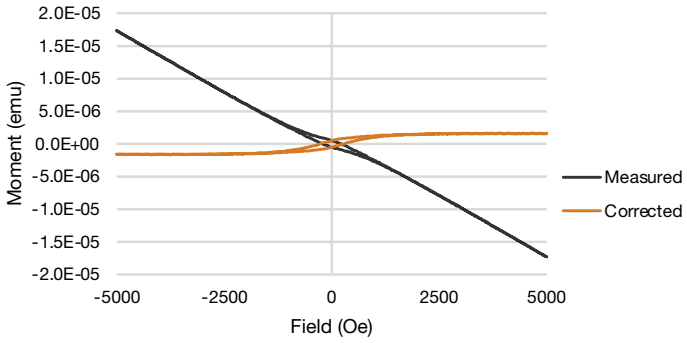

Figure 5:
Fe-doped (0.5%) SiN (2 mm) MHL (measured and linearly corrected) at 2 s averaging.

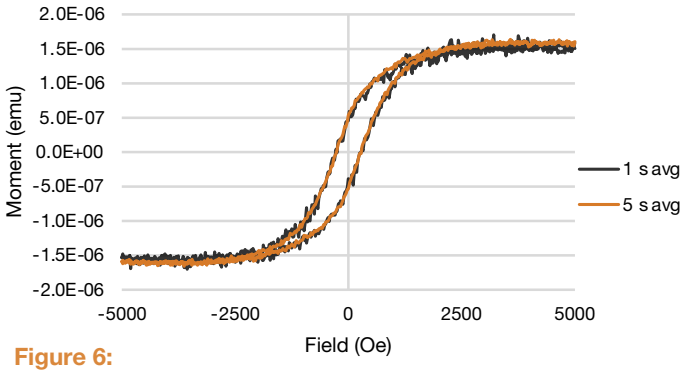

Figure 6:
Fe-doped (0.5%) SiN (2 mm) MHLs (linearly corrected) at 2 s and 5 s averaging.

C. 600 nemu (6 × 10^{-10} Am^2) Fe-doped (0.5%) SiN ceramic sphere (0.8 mm diameter; gap 1):

Figure 7 shows the linearly corrected MHL recorded at gap 1 to ±5 kOe (0.5 T) in equal field increments of 40 Oe (4 mT) at 10 s averaging. Note that full scale is only ±800 nemu (8 × 10^{-10} Am^2).

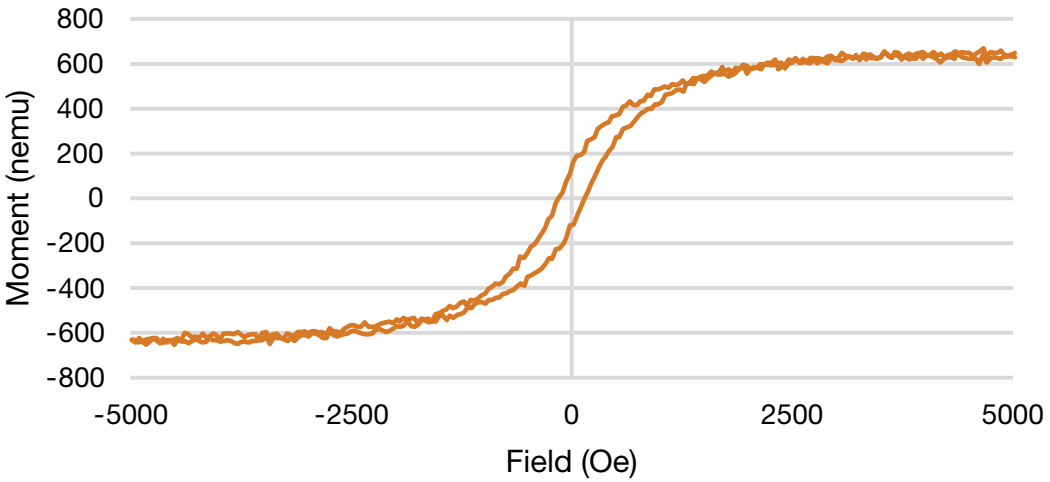

Figure 7:
Fe-doped (0.5%) SiN (0.8 mm) MHL (linearly corrected) at 10 s averaging.

Summary

In this application note, we have presented ambient temperature measurement results for samples with very low magnetic moments, thus demonstrating the sensitivity of the 8600 VSM. MHL and FORC results for a 5.8 µemu (5.8×10^{-9} Am^2) CoPt thin film, and MHL results for 1.5 µemu (1.5×10^{-9} Am^2) and 600 nemu (6×10^{-10} Am^2) Fe-doped (0.5%) SiN ceramic spheres have been presented.

Supplementary information — positioning low-moment samples in the VSM saddle point

Positioning (x, y, z) very low-moment samples in the VSM saddle point can be very challenging, if not impossible, owing to the samples' very low moment and because the diamagnetic or paramagnetic signals from the VSM sample holder are often much greater than the signal from the sample.

In such cases, affix a sample with a higher magnetic moment that has approximately the same dimensions as the sample to be measured to the sample holder to be used, and use this to determine the saddle point. This sample is then removed, and the test specimen sample can be attached. Any minor variations in sample geometries (e.g., thickness) can then be compensated by adjusting the z-position of the sample rod/holder in the magnet gap. A piece of magnetic tape is a convenient sample to use to locate the saddle point because it typically has moments on the order of tens of memu and can be easily cut to approximately the same dimensions as the test specimen.

A small gap (gap 1) bottom-mount quartz sample rod (86-IS-0938) was used for both the CoPt thin film and Fe-doped SiN samples. For the CoPt sample, a small piece of magnetic tape was attached to the sample rod using vacuum grease to determine the saddle point. The magnetic tape was then removed, and the CoPt sample was attached to the same rod using vacuum grease for the MHL measurements shown in Figures 2 and 3, and the FORC measurements shown in Figures 4a and 4b. For the Fe-doped SiN ceramic sphere samples, the samples were attached (varnished) to the sample rod, and a small piece of magnetic tape was then attached to the bottom of the SiN spheres using vacuum grease to determine the saddle point. The tape was then removed, and the z-position of the samples were moved downwards half their diameters (1 mm and 0.4 mm) for the MHL measurements shown in Figures 5, 6, and 7.

References

[1] *B. C. Dodrill, J. R. Lindemuth, Vibrating Sample Magnetometry, in Magnetic Measurement Techniques for Materials Characterization, Spinger Nature, 2021.*

[2] *National Institute of Standards & Technology (NIST) standard reference materials (SRM) 772a (Ni) and 2853 (YIG).*

[3] *I. D. Mayergoyz, Mathematical Models of Hysteresis and their Applications, 2nd Ed., Academic Press, 2003.*

[4] *C. R. Pike, A. P. Roberts, K. L. Verosub, Characterizing Interactions in Fine Magnetic Particle Systems Using First Order Reversal Curves, J. Appl. Phys., 85, 6660,1999.*

[5] *A. P. Roberts, C. R. Pike, K. L. Verosub, First-Order Reversal Curve Diagrams: A New Tool for Characterizing the Magnetic Properties of Natural Samples, J. Geophys. Res., 105, 461, 2000.*

[6] *R. Egli, Magnetic Characterization of Geological Materials with First Order Reversal Curves, in Magnetic Measurement Techniques for Materials Characterization, Springer Nature, 2021.*

[7] *A. Stancu, Characterization of Magnetic Nanostructures with the First Order Reversal Curves Diagram Technique, in Magnetic Measurement Techniques for Materials Characterization, Springer Nature, 2021.*

[8] *D. Gilbert, FORC Diagrams in Magnetic Thin Films, in Magnetic Measurement Techniques for Materials Characterization, Springer Nature, 2021.*

[9] *S. Okamoto, Permanent Magnet Materials, in Magnetic Measurement Techniques for Materials Characterization, Springer Nature, 2021.*

[10] *Y. Cao, M. Ahmadzadeh, K. Xe, B. Dodrill, J. McCloy, Multiphase Magnetic Systems: Measurement and Simulation, J. Appl. Phys., 123(2), 023902, 2018.*

[11] *V. Franco, Magnetocaloric Characterization of Materials, in Magnetic Measurement Techniques for Materials Characterization, Springer Nature, 2021.*

[12] *R. J. Harrison, J. M. Feinberg, FORCinel: An Improved Algorithm for Calculating First-Order Reversal Curve Distributions Using Locally Weighted Regression Smoothing, Geochemistry, Geophysics, Geosystems, 9, 11, 2008.*

[13] *R. Egli, VARIFORC: An Optimized Protocol for Calculating Non-regular First-Order Reversal Curve (FORC) Diagrams, Global and Planetary Change, 203, 110, 203, 2013.*

[14] *B. C. Dodrill, H. S. Reichard, T. Shimizu: Real-Time FORC (RTForc™) Software for the 8600 Series VSM, Technical Note, 2021.*

050923

Questions? Answers?

Visit https://forums.lakeshore.com/
and become part of the conversation!